石墨烯打开带隙研究进展

徐小志, 余佳晨, 张智宏 and 刘开辉

Articles you may be interested in

石墨烯三维骨架结构—合成、性质及应用
国家科学评论 **2**, 40 (2015);

稀有的二维狄拉克材料
国家科学评论 **2**, 22 (2015);

Recent advances in nanoporous graphene membrane for gas separation and water purification
Science Bulletin **60**, 1807 (2015);

铜表面化学气相沉积石墨烯的研究进展：生长行为与控制制备
科学通报 **57**, 2158 (2012);

石墨烯基三维导电网络结构储能电极材料的研究进展
中国科学：化学 **46**, 1110 (2016);

石墨烯打开带隙研究进展

徐小志[†], 余佳晨[†], 张智宏[†], 刘开辉[*]

北京大学物理学院, 北京 100871
* 联系人, E-mail: khliu@pku.edu.cn
† 同等贡献

摘要 石墨烯自从被发现以来, 迅速引发了科学家的研究热潮. 在石墨烯的诸多优异性质中, 超高的电子迁移率使它在未来电子学产业中具有极大的应用前景. 但是石墨烯是零带隙材料, 极大地限制了它在电子学器件上的应用. 在过去几年中, 科学家不断从理论和实验上探索石墨烯打开带隙的方法, 本文以是否直接破坏石墨烯的晶格或化学结构为依据, 从两大类综述了石墨烯打开带隙的理论、计算和实验工作.

关键词 石墨烯, 打开带隙, 场效应晶体管

石墨烯是一种由 sp^2 杂化的碳原子组成的二维蜂窝状材料, 最开始物理学家认为这种材料并不存在(热扰动导致二维材料不稳定). 2004年, 英国曼彻斯特大学 Novoselov 等人[1,2]发现石墨烯不仅可以稳定地存在于衬底上, 而且表现出优越的物理性质. 这一发现迅速引发了广泛的研究热潮, 石墨烯的其他优异性质也逐渐被发现. 实验上测量的石墨烯的电子迁移率高达 350000 $cm^2/(V\ s)$[3], 可观测到室温量子霍尔效应[2]. 石墨烯的力学强度是目前已知的材料当中最强的, 杨氏模量可高于 1 TPa[4]. 同时, 石墨烯还具有超高的导电性、导热性和透光性.

石墨烯具有优异的电学性质, 是制造电子学元件的理想材料. 除此之外, 石墨烯的的制备技术在过去十几年里取得了极大提高[5~7], 为石墨烯的工业化生产与应用奠定了基础. 然而, 由于石墨烯是零带隙材料, 用其制成的场效应晶体管(FET)的通断不能通过栅极控制, 使它无法被应用到现今的电子工业中[8]. 具有理想高开关比的FET需要在室温下有可观的带隙, 例如硅具有约 1.12 eV 的带隙(300 K). 因此, 在室温下打开一个可观的带隙, 同时又不破坏石墨烯本身优异的电学性质, 从而能利用石墨烯制成超越硅的具有更低能耗、更高速度的电子元件, 成为人们长期关注的问题之一.

本文将综述石墨烯打开带隙的理论、计算和实验工作. 本文从机制的角度, 将石墨烯打开带隙的方法大致分为两大类: 一类是直接破坏本征石墨烯的晶格或化学结构, 从而影响其电子性质, 打开带隙, 属于这一类型的方法包括掺杂、吸附原子、引入周期性缺陷、引入限制等. 另一类则不直接破坏石墨烯的六边形晶格结构, 而是通过引入外场、衬底等影响破坏石墨烯的对称性, 从而打开带隙. 除此之外, 利用自旋轨道耦合效应、外加应力、以及考虑石墨烯本征的电子多体效应, 也具有打开带隙的潜力, 它们也被归入第二大类中. 事实上, 许多理论和实验上打开石墨烯带隙的方法均涉及到诸多不同机制的组合, 因此上述分类并非是严格的.

1 石墨烯的基本性质

石墨烯是碳单质同素异形体的一种. 它只有单原子层厚, 即单层的石墨, 具有正六边形的晶格结构

(图1(a)). 在这种六边形的晶格结构中, 相邻的A, B 两个碳原子并不等价, 因此石墨烯的原胞中有2个碳原子, 其实空间晶格基矢为指向2个次近邻碳原子的矢量. 碳原子的4个外层电子当中, 3个电子由sp²杂化形成σ键并与周围的3个碳原子成键, 另外1个电子则为非局域的π电子, 与石墨烯高迁移率、高导电性及其他新奇与优良的电学性质有密切联系.

石墨烯的第一布里渊区为六边形. 与实空间不同的是, 其倒格矢为指向最近邻倒格点的矢量. 石墨烯的能带结构可以用简单的紧束缚近似方法得到. 如果我们仅计入最近邻碳原子的相互作用, 假定最近邻碳原子间π电子的交叠积分为$u(\delta)$, 那么其紧束缚近似下的能带结构应为

$$E(\boldsymbol{k}) = \pm u(\delta)\left|1+e^{i\boldsymbol{k}\cdot\boldsymbol{R}_1}+e^{i\boldsymbol{k}\cdot\boldsymbol{R}_2}\right|, \quad (1)$$

其中$\boldsymbol{R}_1$, $\boldsymbol{R}_2$为晶格矢. $E(\boldsymbol{k})=0$的解恰好是布里渊区6个顶点, 它们被称为狄拉克点, 一般记作$\boldsymbol{K}$和$\boldsymbol{K}'$, 对应两个不等价的倒格点. 在这6个谷对哈密顿量做低能展开, 可以发现其对于$\boldsymbol{q}=\boldsymbol{k}-\boldsymbol{K}(\boldsymbol{K}')$具有线性色散关系, 并且上下支在狄拉克点简并(图1(b)), 这种能带结构被称为狄拉克锥[9]. 由于具有线性的能量色散关系, 石墨烯中的电子具有相对论性电子的性质, 是一种无质量的狄拉克费米子.
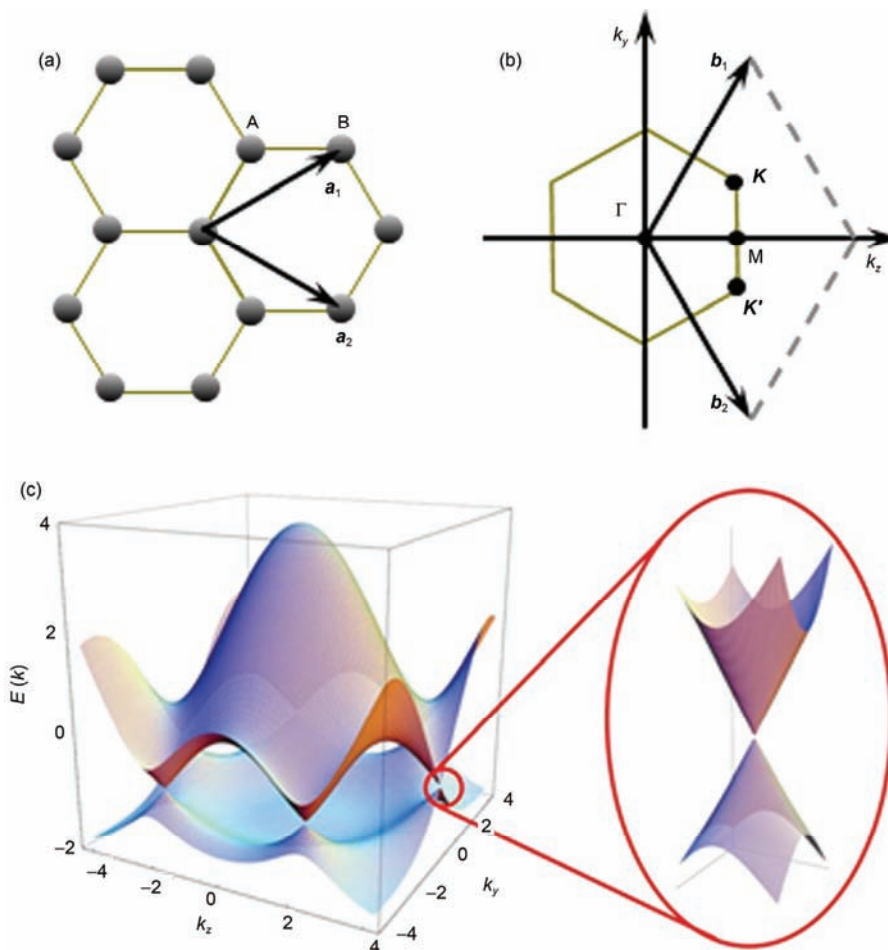
2 破坏石墨烯的晶格或化学结构打开带隙

如前所述, 石墨烯的狄拉克锥型能带结构来源

图1 (网络版彩色)石墨烯的基本性质. (a) 石墨烯的原子结构示意图, 其中A, B是两个不等价碳原子, $\boldsymbol{a}_1$, $\boldsymbol{a}_2$是石墨烯晶格的两个基矢. (b) 石墨烯的倒空间结构, 图中正六边形即第一布里渊区, $\boldsymbol{K}$与$\boldsymbol{K}'$为两个不等价谷, $\boldsymbol{b}_1$, $\boldsymbol{b}_2$是两个倒格矢. (c) 石墨烯的能带结构, 插图即狄拉克锥形能带结构, 每个狄拉克锥的简并点位于第一布里渊区的 6 个角顶点[9]

Figure 1 (Color online) Basic properties of graphene monolayer. (a) The hexagonal lattice structure of graphene, in which A, B atoms are two inequivalent carbon atoms, and $\boldsymbol{a}_1$, $\boldsymbol{a}_2$ are two lattice basis vectors. (b) The hexagonal first Brillouin zone, where $\boldsymbol{K}$ and $\boldsymbol{K}'$ are two valleys and $\boldsymbol{b}_1$, $\boldsymbol{b}_2$ are two reciprocal lattice vectors. (c) Graphene's band structure. The inset shows the Dirac conical dispersion at six corners of hexagonal Brillouin zone[9]

于其自由π电子, 即sp²杂化. 当这种sp²杂化的化学结构被改变时, 能带结构必然会受到相应的影响. 相应地, 石墨烯的几何结构也可能出现改变, 进而打破石墨烯本征的对称性. 这些机制共同导致了石墨烯带隙的打开.

2.1 通过引入掺杂打开带隙

掺杂将直接破坏石墨烯的化学结构, 但有效地打开带隙需要使掺杂呈一定的几何规律性. 理论计算表明, Si, P, S[10], 小范围的BN区域(domain)掺杂[11], CrO_3[12], BN分子[13], 以及p-n双掺杂(如$FeCl_3$受主和K施主[14]), B/N[15,16]均可以打开一定的带隙. 除了直接掺杂外, 外延生长于衬底上的石墨烯也可能受衬底影响而被掺杂(如SiC(0001)), 从而打开带隙[17].

2.2 通过吸附原子打开带隙

原子吸附包括化学吸附和物理吸附两种, 其中, 化学吸附直接与石墨烯中的碳原子成键, 而物理吸附的原子与石墨烯通过分子间作用力联系在一起, 为简便起见, 在这里一并讨论.

最常见的化学吸附原子为氢, 即氢化过程. 早期第一性原理计算结果表明[18], 完全饱和的氢化(分子式CH, 石墨烷), 氢原子在石墨烯两侧与碳原子成键, 碳原子呈sp³杂化, 此时可打开超过3.5 eV的带隙. 图2(a)给出了石墨烷的空间结构示意图, 其中白色的球代表吸附的氢原子, 每个碳原子呈sp³杂化. 图2(b)给出密度泛函理论(DFT)计算给出的态密度谱, 在约3.5 eV的范围内, 态密度均为零, 即石墨烯被打开了一定的带隙. 但是, 尚未有实验工作证实此预言. 其后, 在石墨烯-铱(111)衬底形成的摩尔超晶格上(Moiré superlattice), 实验人员通过不完全氢化, 使氢原子按一定空间周期性覆盖石墨烯部分表面, 打开了数百meV的带隙. 图2(c)给出了扫描隧道显微镜(STM)测得的Ir(111)上石墨烯形成的摩尔超晶格结构图像. 图2(d)是石墨烯暴露于氢气气氛30 s后的表面形貌图, 可以看出氢原子优先吸附在摩尔超晶格上. 图2(e)给出了长时间氢气处理后石墨烯的角分辨光电子能谱(ARPES), 其横轴对应以K为中心、垂直于K与Γ的连线. 自费米能级以下0.4 eV的范围内石墨烯发光强度很弱, 态密度极低[19]. 打开带隙的具体大小取决于氢处理的时长与氢的覆盖模式(pattern), 有

理论计算指出了类似结果[21]. Au衬底上氢化的准悬浮石墨烯被观测到约8%的覆盖, 并打开了1 eV的带隙[22]. 实验表明越大的氢覆盖面积伴随着越大的带隙[23]. 其后, 研究人员实现了在衬底上石墨烯的单侧"石墨烷", 使石墨烯成为绝缘体[24]. 近期, 研究人员利用STM直接观测到了规律性的氢原子吸附[20], 并发现了3种周期模式, 图2(f)~(g)给出了其中两种不同的覆盖模式. 图2(h)给出了在一定氢吸附模式下扫描隧道谱(STS)的结果, 直接证实了带隙中零态密度的特征. 实验证实了3种不同构型的氢吸附分别打开了0.6, 3.4和3.6 eV的带隙.

除氢外, 在石墨烯-铱(111)衬底超晶格上吸附Na原子被观测到可以为石墨烯打开740 meV的带隙[25]. 实验结果表明, 在较弱的氢化处理下, 石墨烯的自旋轨道耦合可以增大3个数量级[26]. 自旋轨道耦合效应可以打开石墨烯带隙(具体讨论见后). 在Fe(110)表面的石墨烯用金原子进行物理吸附, 依靠增强自旋轨道耦合打开了230 meV的带隙[27]. 此外, 理论预测用5d原子作为吸附原子可以使石墨烯打开带隙成为拓扑绝缘体[28].

2.3 通过引入周期性缺陷打开带隙

适当地引入周期性缺陷可以打开石墨烯的带隙. 例如, 理论计算表明[29], 通过引入周期性的单个p_z轨道缺陷, 当缺陷也形成$n×n$的正六边形周期结构时, 可以在石墨烯中形成超晶格结构, 并打开带隙. 图3(a)给出了因缺陷而形成的超晶格结构, 黑色的点代表缺陷, 此处超晶格的边长$n=4$, 记为(4, 0)超晶格. 图3(b)给出了(14, 0)超晶格的示意图, 图中正六边形即超晶格的维格那-塞茨(Wigner-Seitz)原胞, 箭头为两个格矢. 其带隙大小约正比于$1/n^2$, 且不破坏石墨烯的点群对称性. 如图3(c)~(h)所示, 引入更大的具有周期性的缺陷[31,32], 可以在打开带隙的同时使石墨烯比碳纳米带具有更优良的导电性和大致相当的开关比. 图3(c)~(e)为正六边形缺陷形成的超晶格示意图, L, R分别给出了超晶格的晶格常数和缺陷大小. 图3(f)给出了实现该种结构的化学处理手段. 首先蒸镀硅氧化物作为保护层和旋涂高分子有机物, 有机物层在退火后会形成多孔结构, 成为纳米筛(nanomesh)的天然模板. 图3(g), (h)为刻蚀后石墨烯的透射电子显微镜(TEM)图像, 有理论工作将此效应解释为缺陷带来的手征对称性的破缺[33].
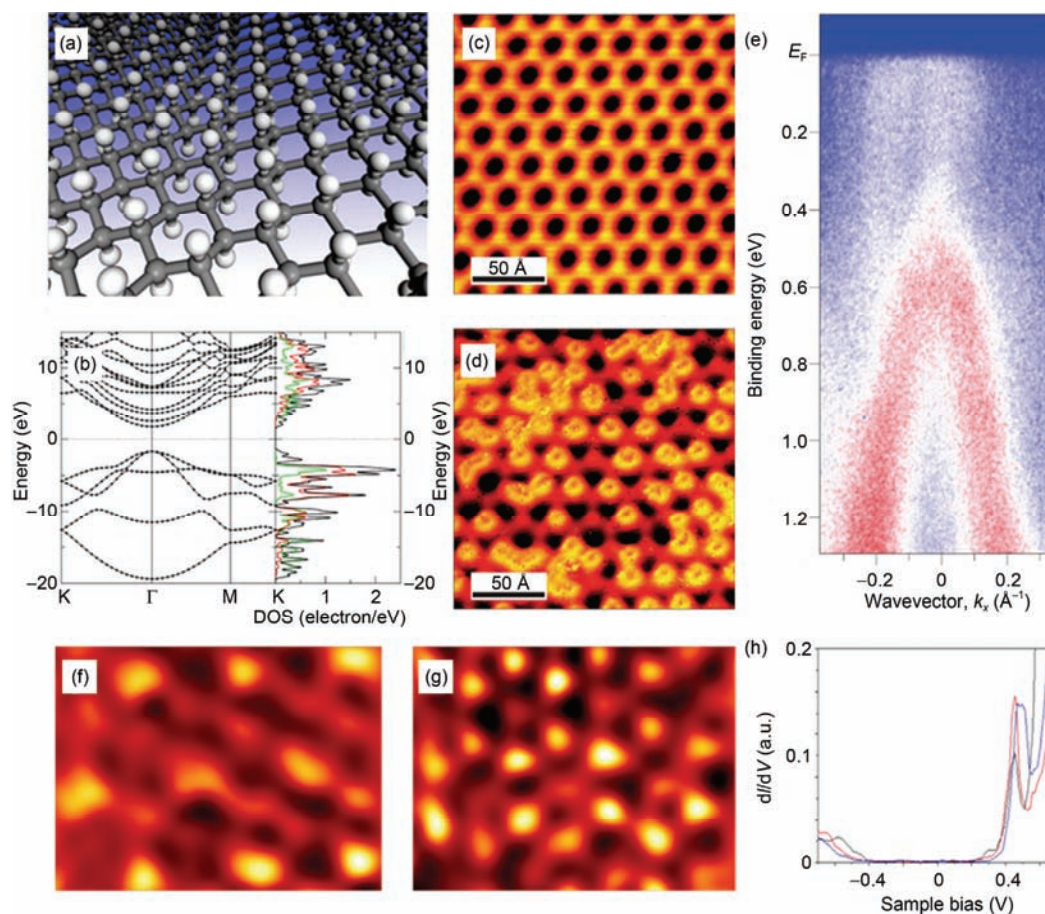
图 2 (网络版彩色)氢化石墨烯打开带隙. (a) 完全氢化石墨烯(石墨烷)呈sp³杂化, 图中白色和灰色球分别代表氢原子和碳原子. (b) 理论计算得到的完全氢化石墨烯的能带结构和态密度[18]. (c), (d) 氢气处理前后, Ir(111)表面石墨烯的STM图. (e) 氢气处理后的石墨烯的ARPES[19]. (f), (g) 用化学气相沉积(CVD)方法生长在铜箔表面的石墨烯经氢气处理后的两种可能的氢吸附模式(STM图). (h) 氢吸附后的STS测量结果证实了打开带隙[20]

Figure 2 (Color online) Hydrogenated graphene and gap opening. (a) Schematic of fully-hydrogenated graphene (graphane) showing sp³ hybridization. The white and gray spheres shown in the figure represent H and C atoms respectively. (b) Theoretical band structure and density of states for graphane[18]. (c), (d) STM images of graphene on Ir(111) superlattice before and after hydrogenation. (e) ARPES result after hydrogenation verifying the presence of band gap[19]. (f), (g) Two possible patterns of hydrogenated CVD growth graphene on copper foil (STM image). (h) STS measurement showing band gap after hydrogenation[20]

2.4 通过引入限制打开带隙

引入量子限制将有效地改变石墨烯的能带结构, 打开带隙. 一种最常见的量子限制是在一个方向上使石墨烯只有很小的宽度, 即形成碳纳米带(graphene nanoribbon, GNR). 在被限制的方向上, 准动量只能取分立的值.

早期基于简单紧束缚近似和直接求解无质量费米子狄拉克方程的计算结果认为[34,35], 扶手椅型(armchair)边界碳纳米带随宽度变化可呈现金属、绝缘行为, 而之字型(zigzag)边界无论任何宽度均呈金属性. 图4(a)为扶手椅型边界, 图4(b)为之字型边界,

图中箭头表示纳米带的延展方向. 随后, 更精细的第一性原理计算同时考虑到量子限制效应和边界效应, 认为在两种边界条件下均可打开带隙[36]. 图4(c), (d)给出了之字形边界下基于紧束缚(图4(c))和第一性原理的局域密度近似(LDA)方法(图4(d))计算得到的带隙随纳米带宽度的变化, N_a为沿之字形边界方向正六边形原胞的个数. 随着纳米带长度的不同(原胞个数的不同), 纳米带的带隙会有显著区别. 随后, 实验观测证实了碳纳米带打开带隙的行为[37~39], 并且在10 nm宽度以下实现了具有较高开关比的FET. 对于双层石墨烯, 实验同样证实了带状量子限制会打开
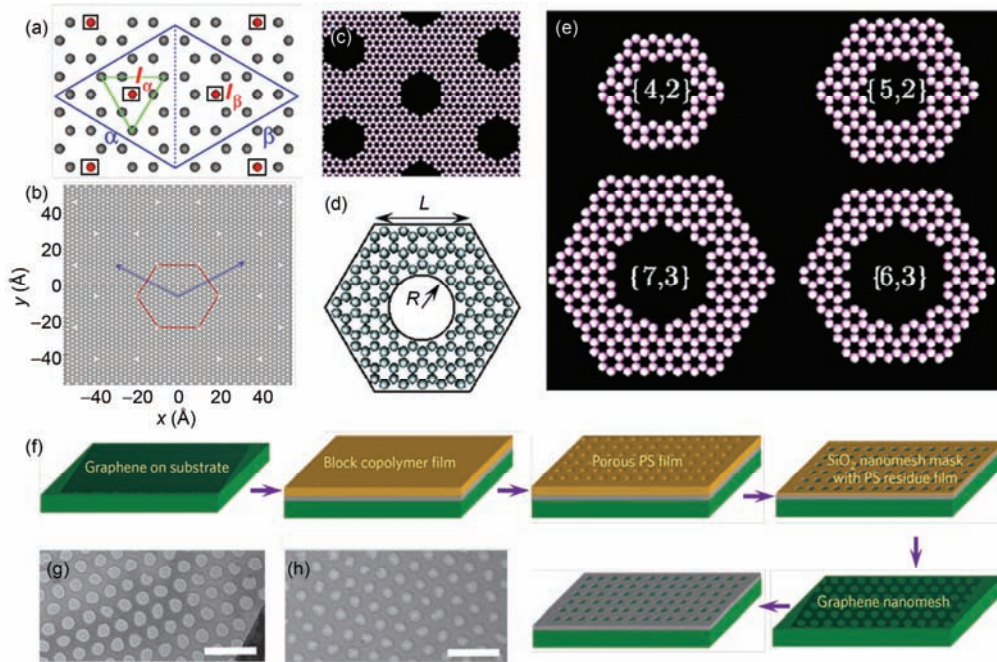
图3 (网络版彩色)周期性缺陷打开石墨烯带隙. (a) p$_z$轨道缺陷形成的n=4 超晶格，方框内圆点表示缺失的p$_z$轨道，黑色圆点为碳原子. (b) n=14 超晶格，箭头为两个独立晶格矢，正六边形为Wigner-Seitz原胞[29]. (c)~(e) 石墨烯中形成具有同样对称性的周期性缺陷结构(antidot)[30]，L和R分别表示超晶格原胞的边长和缺陷的半径[31]. (f) 石墨烯空间周期性缺陷结构(graphene nanomesh)的一种化学加工方法示意图[32]. (g), (h) 加工后的TEM图像，具有不同的缺陷大小和间距. 比例尺, 100 nm

Figure 3 (Color online) Periodic defects: p$_z$ orbital missing, antidots and nanomesh. (a) Superlattice formed by missing p$_z$ orbital in graphene. The dots with frame denote missing orbitals whereas the dots denote graphene atoms. (b) Superlattice with perodicity n=14. Two arrows represent lattice vectors, and the hexagon is the superlattice Wigner-Seitz unit cell[29]. (c)–(e) Periodic antidots in graphene with hexagonal symmetry[30]. L and R denote superlattice unit cell size and antidot radius, respectively[31]. (f) A schematic of the chemical processing method for graphene nanomesh[32]. (g), (h) TEM images after processing with various antidot size and unit cell size. Scale bar, 100 nm
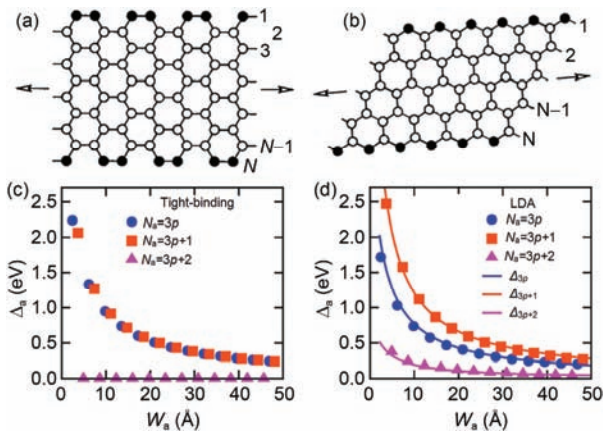

图4 (网络版彩色)石墨烯纳米带. (a), (b) 扶手椅/之字形边界的石墨烯纳米带示意图. 箭头表示纳米带的延伸方向，数字表示纳米带的横向原子数[34]. 基于紧束缚近似(c)和LDA方法(d)计算得到的之字形边界下带隙-纳米带宽度关系，N_a表示纳米带边界上的原子个数[35]

Figure 4 (Color online) Graphene nanoribbon. (a), (b) Schematic of armchair/zigzag edge graphene nanoribbon. Arrows denote translational directions[34]. Band gap width-dependence of zigzag-edged GNR, obtained by calculations based on tight-banding (TB) (c) and LDA (d). N_a denotes number of atoms on the edge[35]

带隙[40]. 但这种机制的问题在于，纳米带打开的带隙与其具体宽度、几何、边界等有较为复杂的依赖关系[37~39,41]，使其实际应用困难重重. 类似的，将石墨烯制成量子点打开带隙也已被实验证实[42].

3 不破坏石墨烯的晶格或化学结构打开带隙

在狄拉克点附近，哈密顿量的有效形式为：

$$H = \vec{h}(\boldsymbol{k}) \cdot \vec{\sigma}, \tag{2}$$

其中 $\vec{\sigma}$ 为赝自旋的泡利矩阵. 对于无质量狄拉克费米子，我们有$h_z(\boldsymbol{k})$=0，此时电子具有线性能量色散关系，而参数$h_z(\boldsymbol{k})$的物理意义即相对论性电子的"有效质量"参数. 从对称性的角度考虑，A/B亚晶格对称要求$h_z(\boldsymbol{k})$=$-h_z(\boldsymbol{k})$，时间反演对称要求$h_z(\boldsymbol{k})$=$h_z(-\boldsymbol{k})$，即h_z=0. 由于体系具有C$_6$旋转对称性，空间反演对称性等价于A/B亚晶格对称性. 简单来看，破坏亚晶格或时间反演对称性似乎是打开带隙的必要条件. 大多

数情况下, 打开带隙的同时伴随着这两种对称性的破缺, 在一些特殊情形下, 可以在打开带隙的同时保持这两种对称性.

3.1 通过加外场打开带隙

通过加外场可以直接打破石墨烯的时间反演对称性或空间反演对称性, 从而打开石墨烯的带隙. 一种最直接的方式是加垂直于石墨烯平面的磁场. 此时, 石墨烯中的近自由电子会形成朗道能级, 即分立的量子化能级, 电子由低到高填充这些朗道能级. 从能带的意义上讲, 这使石墨烯成为了一种特殊的绝缘体.

事实上, 外加磁场破坏石墨烯的时间反演对称

性并打开带隙, 并非人们提出的唯一打开带隙的机制. 1988年, Haldane[43]提出了被称为"Haldane模型"的玩具模型, 通过在石墨烯原胞中加入总和为零的周期性磁通, 破坏了石墨烯的时间反演对称性, 使石墨烯成为具有非平庸拓扑性质的绝缘体, 同时与量子霍尔效应一样, 有手征边界态存在.

对于双层和三层石墨烯, 诸多理论和实验工作表明, 施加垂直方向的电场可以打开带隙, 并且带隙的大小随外加电场的强弱可调[44~48]. 这种可调带隙可以用紧束缚近似做很好的估计. 图5(a)是ABC-堆叠的三层石墨烯光电导-门电压依赖关系测量结果. 图5(b)是紧束缚近似下三层石墨烯的能带结构, 其中
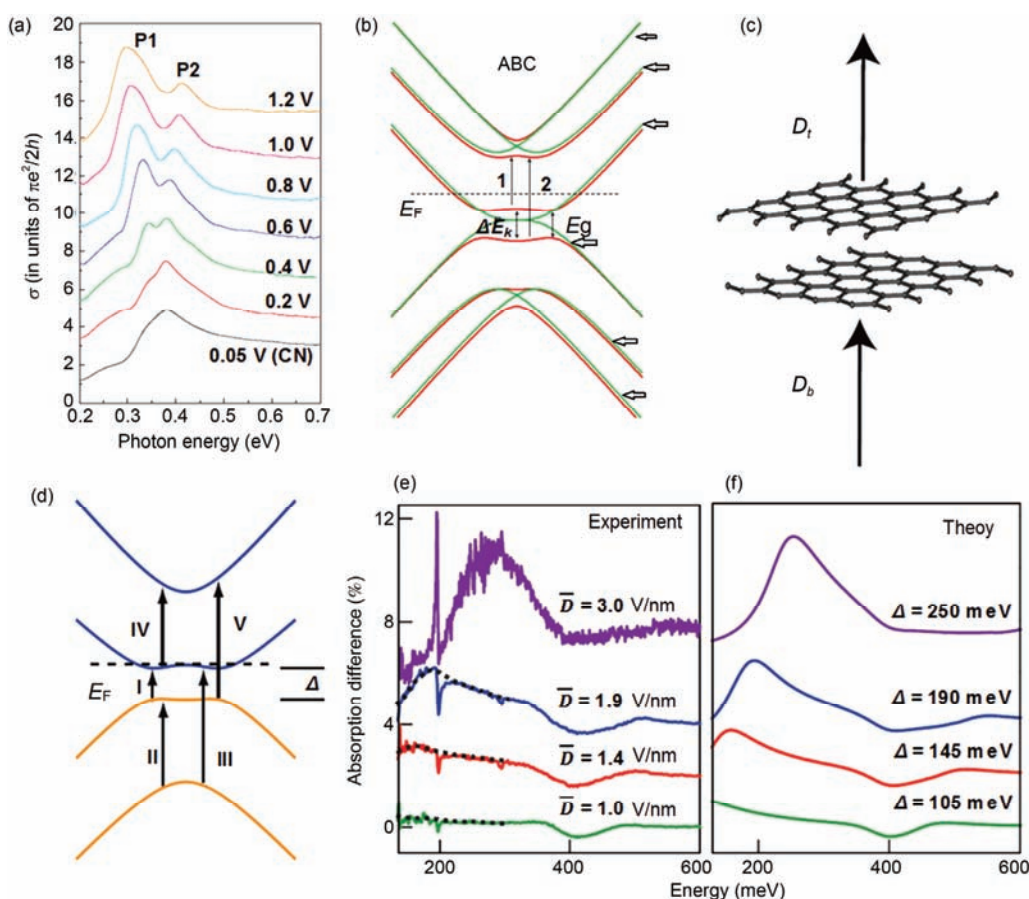

图 5 (网络版彩色)双层、三层石墨烯带隙的垂直外电场调控. (a) 三层石墨烯的光电导-外加垂直电压关系图. 峰P1, P2代表的光激发过程对应于(b)中的过程1, 2. (b) 紧束缚近似下外加电场时石墨烯能带结构示意图. 箭头指向的线表示紧束缚近似下无外场的能带结构[44]. (c)~(f) 双层石墨烯通过红外吸收谱测量带隙与外加垂直电场关系. (c) 外电场分布示意图. (d) 紧束缚近似给出的外加电场下能带结构. (e), (f) 实验测量和理论计算得到的吸收峰随外电压的变化, 其中主峰对应(d)中的I过程, (e)中虚线为峰位示意[48]

Figure 5 (Color online) Gate tunable band gap in bilayer and trilayer graphene. (a) Photoconductance-gate voltage relation, in which peak P1 and P2 correspond to excitation processes 1 and 2 in (b), respectively. (b) TB band structure with and without applying gate voltage[44]. (c)–(f) Infrared absorption spectrum with varying gate voltage. (c) Schematic for the displacement field distribution. (d) Band structure obtained by TB calculation with gate voltage applied. (e), (f) Experiment and theory results showing gate dependent absorption peak position, which indicates energy gap for the excitation I in (d). Dashed lines in (e) are guides to the eye[48]

浅灰色对应无外加垂直电场，黑色对应外加垂直电场，1，2对应最强的两个光跃迁信号，即图5(a)中的P1，P2峰。随着外加垂直电场的增强，两个峰的能量劈裂随之增大，意味着带隙的打开。图5(c)~(f)为双层石墨烯外加垂直电场下的红外光谱测量结果。图5(c)为双层石墨烯门电压的分布，在门电压作用下，双层石墨烯会打开带隙，同时费米能级相应地移动。图5(e)，(f)显示了测量结果与理论计算结果，其峰对应的是图5(d)中I跃迁过程。随外加电压增大，双层石墨烯的带隙有显著增大。然而，对于单层石墨烯，一般用同样的方式不能打开带隙。但计入自旋轨道耦合作用后，外加电场带来的Rashba效应(二维电子气中，当考虑自旋轨道耦合并有垂直平面方向上的反演对称性破缺，例如外加垂直电场，会带来一种动量依赖的自旋劈裂效应)，经过其他机制的加强后，可以打开石墨烯的带隙，详细讨论见后。有报道指出受衬底影响的石墨烯可能具有门电极可调的带隙[49,50]。

此外，基于研究电光相互作用的Floquet理论(求解具有时间周期性动力系统的线性微分方程的一种方法)，光与石墨烯相互作用的理论工作表明，光激发具有打开石墨烯带隙的潜力[51]。

3.2 通过衬底影响打开带隙

衬底可以通过直接打破石墨烯的A/B亚晶格对称性打开带隙。通常，通过外延生长于衬底上的石墨烯容易受此机制的影响。最简单的机制是通过使A，B原子感受到不同的化学势而打开带隙。此外，规律

性地与衬底成键，或石墨烯与衬底之间的电荷转移过程也可以起到相同的效果。例如，Zhou等人[52]发现在SiC上外延生长的石墨烯与衬底之间会形成由碳原子构成的缓冲层，使有且仅有石墨烯的A原子直接位于缓冲层的碳原子之上。随后，他们用ARPES证实了石墨烯打开带隙的行为。图6(a)~(c)分别对应单层、双层、三层石墨烯的ARPES测量结果，横轴为以K谷为中心、垂直于K与Γ的连线。结果表明，随着层数增大，带隙逐渐减小[52]。尽管在单层石墨烯中观察到了与有质量狄拉克费米子非常接近的色散关系(图6(a))，但其"带隙"内非零的态密度却是十分反常的，因此是否真正打开了单层石墨烯的带隙仍有争议。此外，外延生长在SiC[53~55]，g-C$_3$N$_4$[56,57]，hBN[58]等衬底上的石墨烯均被预言或证实有打开带隙的行为。另一种常见的机制是衬底通过表面重构形成和石墨烯类似的正六边形周期结构，从而破坏A/B对称性打开带隙，包括SiC[59~61]，Cu[62]，MgO[63]，Al$_2$O$_3$[64]等。

3.3 通过衬底形成摩尔条纹打开带隙

当石墨烯与hBN形成范德瓦尔斯异质结时，如果两者的六边形晶格具有较小的相对偏转角度，由于hBN与石墨烯有微小的晶格常数差别，它们便会形成周期性的摩尔条纹(Moiré pattern)，如图7(a)所示，也被称为摩尔超晶格。最近的实验表明，这种结构会为石墨烯打开数十meV的带隙，其大小随超晶格的晶格常数增大而增大[65,66]。图7(a)给出了石墨烯在BN上形成的超晶格示意图。图7(b)，(c)分别为
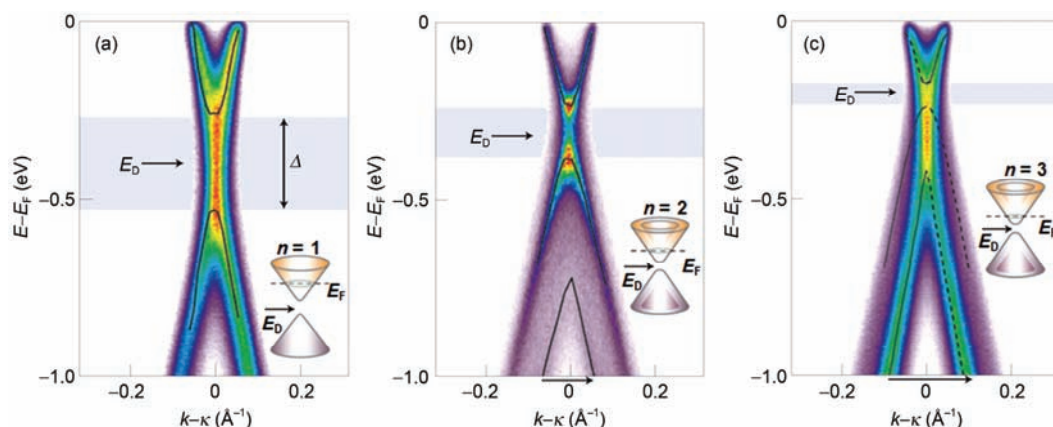

图 6 (网络版彩色)衬底与石墨烯间缓冲层破坏A/B对称性打开带隙。生长于6H-SiC衬底上的单层(a)、双层(b)、三层(c)石墨烯的ARPES测量结果[52]

Figure 6 (Color online) Buffer layer between graphene-SiC opens band gap for graphene. ARPES results for monolayer (a), bilayer (b) and trilayer (c) graphene[52]
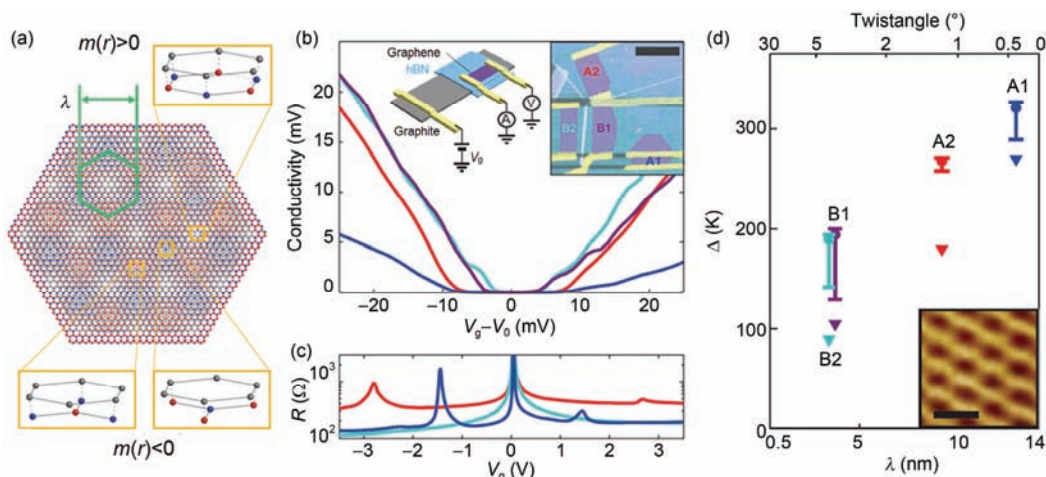
图 7 (网络版彩色)摩尔超晶格打开带隙. (a) 摩尔超晶格的示意图[65]. (b) 150 mK下测得的电中性点附近的电导-门电压关系图. 插图为测量样品的示意图和光学照片. 比例尺: 3 μm. (c) 更大门电压范围的电阻-门电压关系. (d) 摩尔超晶格周期、石墨烯转角与测得带隙的关系. 插图为B2的扫描隧道形貌图. 比例尺: 5 nm

Figure 7 (Color online) Band gap opened by Moiré superlattice. (a) Schematic for the Moiré superlattice[65]. (b) Conductance-gate voltage dependence near charge neutral position (CNP) measured at 150 mK. Inset, measured device and optical image of the device. Scale bar: 3 μm. (c) Resistance-gate voltage dependence at a larger range. Peaks away from CNP are superlattice minibands. (d) Correlation between Moiré pattern wavelength (twist angle) and measured band gap. Inset, scanning tunneling topography image for B2. Scale bar: 5 nm

150 mK下在电中性点附近和更大范围的电导-门电压关系, 除了电中性点附近的带隙外, 还可以看到由摩尔超晶格结构形成的迷你带(miniband)结构. 图7(d)显示了超晶格晶格常数与电中性点附近打开的带隙的正相关行为. 然而, 与之前提到的衬底打开带隙的机制有所不同的是, 此处的hBN虽然破坏了石墨烯空间反演对称性, 但并未直接破坏其A/B对称性, 也不存在电荷转移等其他打开带隙的效应. 最近, 这种打开带隙的方式引起了人们的关注.

从唯象的角度来看, 可以用参数m(r)表征局域的带隙大小. 由于体系具有周期性, m(r)随位置发生周期性的正负震荡, 在空间平均下, 似乎会使带隙消失. 但更细致的理论计算结果表明, 石墨烯整体的带隙并不简单地取决于局域m(r)的简单空间平均[67~73]. 基于不同的理论假设和考虑因素, 通过紧束缚近似或重整群的计算, 研究人员得到不同大小的带隙估计值[67~73]及对相对角度的依赖性.

以上理论和实验均基于石墨烯不发生结构性形变的前提之下. 但是, Woods等人[74]研究表明在较小相对角度下, 石墨烯会被衬底"拉伸"以契合衬底, 并且形成周期性的畴, 其畴壁可能导致石墨烯的绝缘行为. 此外, 他们还在此实验中发现, 由上下两层hBN包裹的石墨烯带隙有显著减小的效应. 最近, Wang等人[75]利用ARPES, 证实了形成摩尔条纹条件

下的石墨烯带隙, 大小比之前的实验观测更大, 达到了160 meV.

3.4 通过自旋轨道耦合效应打开带隙

石墨烯中的自旋轨道耦合(SOC)效应有两种不同的机制[75]: 一种是本征机制, 其哈密顿量为

$$H_{SO} = \Delta_{SO}\sigma_z\tau_z s_z. \tag{3}$$

另一种是由结构反演对称性破缺带来的Rashba自旋轨道耦合机制, 其要求沿z方向有电场, 其哈密顿量为

$$H_{Rashba} = \Delta_R(\sigma_x\tau_z s_y - \sigma_y s_x), \tag{4}$$

其中σ, τ, s分别对应亚晶格赝自旋、谷赝自旋、自旋的泡利矩阵. 本征石墨烯自旋轨道耦合效应极其微弱. 基于考虑σ–π轨道耦合效应的第一性原理计算结果表明, 本征SOC打开约1 μeV的带隙, 而Rashba SOC打开约10 (μeV nm)/V的带隙, 随沿z方向化学势变大而变大[76,77].

从对称性的角度来看, 本征SOC并不破坏石墨烯的任何对称性. 它打开带隙使石墨烯为量子自旋霍尔态, 即其体态是绝缘的, 但具有对称性保护的导电边界态; 著名的Kane-Mele模型最早预言了该效应[76]. 但是, 由于石墨烯的本征SOC极弱, 尚未有实验证实本征SOC带来的这些效应. Rashba SOC同样是

广泛存在的, 因为任何衬底的影响原则上都会打破体系沿垂直石墨烯平面方向的对称性. 通过掺杂、吸附原子、衬底影响等[26,27,54,78]方式, 石墨烯的自旋轨道耦合效应会有显著增强.

3.5 通过外加应力打开带隙

外加应力同样会破坏石墨烯的空间反演对称性. 第一性原理、紧束缚近似计算和密度泛函理论(DFT)计算表明[79~83], 剪应力和单轴应力都有打开带隙的能力. 实验结果证实了通过将石墨烯置于较柔软的衬底上, 衬底可以在一个方向对石墨烯施加单轴应力, 使该方向上的碳碳键变长[84]. 另有理论计算结果表明, 若施加沿3个主要晶向的应力, 其效果相当于一个垂直于石墨烯平面的赝磁场, 从而形成朗道能级打开带隙[85]. 当应力方向分别沿 [100], [010] 和[001]时, 可以导致均匀地等效于数十特斯拉(T)的磁场, 从而打开0.1 eV量级的带隙. 当把较大的石墨烯置于如图8(a)所示的表面时, 其应力在石墨烯内的分布会形成具有更大空间周期的超晶格结构, 进而导致等效磁场如图8(c)所示. 这种周期性的应力可以使石墨烯形成如图8(b)所示的能带结构. 实验上, Levy等人[86]利用扫描隧道显微镜(STM)技术在有很大应变的纳米鼓包上观察到了量子霍尔效应. 该现象说明由于巨大应变的存在, 产生了强度高达300 T以上的赝磁场, 在低温下可以形成朗道能级(图8(d), (e)). 另有报道表明, 施加双轴应力可能带来手征对称性的破缺, 进而打开带隙[33].

3.6 通过电子多体相互作用效应打开带隙

以上理论模型都是基于讨论石墨烯中电子的单体问题. 理论分析结果表明, 在狄拉克点附近, 如果计入长程的电子-电子库伦相互作用, 石墨烯具有自发的打开带隙的行为[87]. 这种自发的质量产生机制与2+1维量子电动力学中的手征对称性破缺有深刻的理论联系. 基于无规相位近似和蒙特卡洛模拟的分析结果表明, 随着库伦相互作用耦合常数的增大, 石墨烯在电中性点附近会发生金属-绝缘体相变. 这种有效质量产生的机制也被称为激子质量产生, 它源于不同谷激子配对行为. 具体来讲, K 谷内的配对行为形成电荷密度波态, 而 K, K' 的配对行为形成凯库勒扭曲(Kekule distortion)态.

除了本征的打开带隙机制外, 电子多体相互作用也会增强上述提到的各种打开带隙机制. 例如, 对于破坏A/B对称性的外势场打开带隙Δ_0, 由Hatree-

图 8 (网络版彩色)应变打开带隙. (a) 产生应变的三重对称性表面. (b) 周期性的应变导致的低能端能带分布. (c) 由于(a)的褶皱导致的赝磁场强度分布, 对应−0.5~0.5 T的强度B_S分布[85]. (d) Pt(111)上石墨烯鼓包的STM形貌图. (e) 横跨石墨烯鼓包得到的STM谱[86]

Figure 8 (Color online) Band gap opened by strain. (a) Strain with triangular symmetry created by depositing graphene on profiled surfaces. (b) Low-energy bands induced by the periodic strain. (c) The distribution of pseudomagnetic field. B_S varies in the range −0.5–0.5 T[85]. (d) STM topography of graphene monolayer on Pt(111) with nanobubbles. (e) STM spectra taken in a line across a graphene nanobubble[86]

Fock 近似和重整化群计算可以得到修正的带隙 $\tilde{\Delta}_0 > \Delta_0$. 电子-电子相互作用也可以对数增大由 SOC 打开的带隙[76].

4 总结与展望

综上所述, 石墨烯具有非常多优异的性能, 具有极大的电子学应用前景, 是未来理想的电子学器件原材料. 但是, 要想真正把石墨烯应用在电子学领域, 制成具有高开关比的石墨烯 FET, 打开石墨烯的带隙是一个基本条件. 经过科学家的不断努力, 很多种基于不同物理机制的打开石墨烯带隙的方法已经被理论预测或实验证实. 但是, 由于打开一个较大带隙对石墨烯的电子性质是一个很大的改变, 因此在保证石墨烯优异的电子学性能不被破坏的前提下, 究竟哪种现有机制或尚未发现的机制, 能够有效、大面积地打开石墨烯的带隙, 保证石墨烯带隙的精确可控, 直至找到大规模工业化生产高质量电子学元件的方法, 仍有待科学家的不断探索和挖掘.

参考文献

1   Novoselov K S, Geim A K, Morozov S V, et al. Electric field effect in atomically thin carbon films. Science, 2004, 306: 666–669

2   Novoselov K S, Jiang Z, Zhang Y, et al. Room-temperature quantum hall effect in graphene. Science, 2007, 315: 1379–1379

3   Banszerus L, Schmitz M, Engels S, et al. Ultrahigh-mobility graphene devices from chemical vapor deposition on reusable copper. Sci Adv, 2015, 1: e1500222

4   Lee C, Wei X D, Kysar J W, et al. Measurement of the elastic properties and intrinsic strength of monolayer graphene. Science, 2008, 321: 385–388

5   Bhaviripudi S, Jia X T, Dresselhaus M S, et al. Role of kinetic factors in chemical vapor deposition synthesis of uniform large area graphene using copper catalyst. Nano Lett, 2010, 10: 4128–4133

6   Li X S, Cai W W, An J H, et al. Large-area synthesis of high-quality and uniform graphene films on copper foils. Science, 2009, 324: 1312–1314

7   Xu X, Zhang Z, Qiu L, et al. Ultrafast growth of single-crystal graphene assisted by a continuous oxygen supply. Nat Nanotechnol, 2016, 11: 930–935

8   Schwierz F. Graphene transistors. Nat Nanotechnol, 2010, 5: 487–496

9   Castro Neto A H, Guinea F, Peres N M R, et al. The electronic properties of graphene. Rev Mod Phys, 2009, 81: 109–162

10 Denis P A. Band gap opening of monolayer and bilayer graphene doped with aluminium, silicon, phosphorus, and sulfur. Chem Phys Lett, 2010, 492: 251–257

11 Fan X F, Shen Z X, Liu A Q, et al. Band gap opening of graphene by doping small boron nitride domains. Nanoscale, 2012, 4: 2157–2165

12 Zanella I, Guerini S, Fagan S B, et al. Chemical doping-induced gap opening and spin polarization in graphene. Phys Rev B, 2008, 77: 073404

13 Shinde P P, Kumar V. Direct band gap opening in graphene by bn doping: *Ab initio* calculations. Phys Rev B, 2011, 84: 125401

14 Yang J W, Lee G, Kim J S, et al. Gap opening of graphene by dual FeCl$_3$-acceptor and k-donor doping. J Phys Chem Lett, 2011, 2: 2577–2581

15 Deng X H, Wu Y Q, Dai J Y, et al. Electronic structure tuning and band gap opening of graphene by hole/electron codoping. Phys Lett A, 2011, 375: 3890–3894

16 Rani P, Jindal V K. Designing band gap of graphene by B and N dopant atoms. RSC Adv, 2013, 3: 802–812

17 Coletti C, Riedl C, Lee D S, et al. Charge neutrality and band-gap tuning of epitaxial graphene on SiC by molecular doping. Phys Rev B, 2010, 81: 235401

18 Sofo J O, Chaudhari A S, Barber G D. Graphane: A two-dimensional hydrocarbon. Phys Rev B, 2007, 75: 153401

19 Balog R, Jorgensen B, Nilsson L, et al. Bandgap opening in graphene induced by patterned hydrogen adsorption. Nat Mater, 2010, 9: 315–319

20 Lin C F, Feng Y X, Xiao Y D, et al. Direct observation of ordered configurations of hydrogen adatoms on graphene. Nano Lett, 2015, 15: 903–908

21 Gao H L, Wang L, Zhao J J, et al. Band gap tuning of hydrogenated graphene: H coverage and configuration dependence. J Phys Chem C, 2011, 115: 3236–3242

22 Haberer D, Vyalikh D V, Taioli S, et al. Tunable band gap in hydrogenated quasi-free-standing graphene. Nano Lett, 2010, 10: 3360–3366

23 Matis B R, Burgess J S, Bulat F A, et al. Surface doping and band gap tunability in hydrogenated graphene. ACS Nano, 2012, 6: 17–22

24 Elias D C, Nair R R, Mohiuddin T M G, et al. Control of graphene's properties by reversible hydrogenation: Evidence for graphane. Science, 2009, 323: 610–613

25 Papagno M, Rusponi S, Sheverdyaeva P M, et al. Large band gap opening between graphene dirac cones induced by Na adsorption onto an Ir superlattice. ACS Nano, 2012, 6: 199–204

26 Balakrishnan J, Koon G K W, Jaiswal M, et al. Colossal enhancement of spin-orbit coupling in weakly hydrogenated graphene. Nat Phys, 2013, 9: 284–287

27 Varykhalov A, Sanchez-Barriga J, Marchenko D, et al. Tunable fermi level and hedgehog spin texture in gapped graphene. Nat Commun, 2015, 6: 7610

28 Hu J, Alicea J, Wu R Q, et al. Giant topological insulator gap in graphene with 5d adatoms. Phys Rev Lett, 2012, 109: 266801

29 Martinazzo R, Casolo S, Tantardini G F. Symmetry-induced band-gap opening in graphene superlattices. Phys Rev B, 2010, 81: 245420

30 Cocco G, Cadelano E, Colombo L. Gap opening in graphene by shear strain. Phys Rev B, 2010, 81: 241412

31 Bai J W, Zhong X, Jiang S, et al. Graphene nanomesh. Nat Nanotechnol, 2010, 5: 190–194

32 Pedersen T G, Flindt C, Pedersen J, et al. Graphene antidot lattices: Designed defects and spin qubits. Phys Rev Lett, 2008, 100: 136804

33 Lee S H, Chung H J, Heo J, et al. Band gap opening by two-dimensional manifestation of peierls instability in graphene. ACS Nano, 2011, 5: 2964–2969

34 Ezawa M. Peculiar width dependence of the electronic properties of carbon nanoribbons. Phys Rev B, 2006, 73: 045432

35 Nakada K, Fujita M, Dresselhaus G, et al. Edge state in graphene ribbons: Nanometer size effect and edge shape dependence. Phys Rev B, 1996, 54: 17954–17961

36 Son Y W, Cohen M L, Louie S G. Energy gaps in graphene nanoribbons. Phys Rev Lett, 2006, 97: 216803

37 Chen Z H, Lin Y M, Rooks M J, et al. Graphene nano-ribbon electronics. Phys E, 2007, 40: 228–232

38 Han M Y, Ozyilmaz B, Zhang Y B, et al. Energy band-gap engineering of graphene nanoribbons. Phys Rev Lett, 2007, 98: 206805

39 Wang X R, Ouyang Y J, Li X L, et al. Room-temperature all-semiconducting sub-10 nm graphene nanoribbon field-effect transistors. Phys Rev Lett, 2008, 100: 206803

40 Szafranek B N, Schall D, Otto M, et al. Electrical observation of a tunable band gap in bilayer graphene nanoribbons at room temperature. Appl Phys Lett, 2010, 96: 112103

41 Barone V, Hod O, Scuseria G E. Electronic structure and stability of semiconducting graphene nanoribbons. Nano Lett, 2006, 6: 2748–2754

42 Ponomarenko L A, Schedin F, Katsnelson M I, et al. Chaotic dirac billiard in graphene quantum dots. Science, 2008, 320: 356–358

43 Haldane F D M. Model for a quantum hall-effect without landau-levels-condensed-matter realization of the parity anomaly. Phys Rev Lett, 1988, 61: 2015–2018

44 Lui C H, Li Z Q, Mak K F, et al. Observation of an electrically tunable band gap in trilayer graphene. Nat Phys, 2011, 7: 944–9475

45 Mak K F, Lui C H, Shan J, et al. Observation of an electric-field-induced band gap in bilayer graphene by infrared spectroscopy. Phys Rev Lett, 2009, 102: 25640

46 Min H K, Sahu B, Banerjee S K, et al. *Ab initio* theory of gate induced gaps in graphene bilayers. Phys Rev B, 2007, 75: 155115

47 Ohta T, Bostwick A, Seyller T, et al. Controlling the electronic structure of bilayer graphene. Science, 2006, 313: 951–954

48 Zhang Y B, Tang T T, Girit C, et al. Direct observation of a widely tunable bandgap in bilayer graphene. Nature, 2009, 459: 820–823

49 Zhu W J, Neumayer D, Perebeinos V, et al. Silicon nitride gate dielectrics and band gap engineering in graphene layers. Nano Lett, 2010, 10: 3572–3576

50 Quhe R G, Zheng J X, Luo G F, et al. Tunable and sizable band gap of single-layer graphene sandwiched between hexagonal boron nitride. NPG Asia Mater, 2012, 4: E6

51 Calvo H L, Pastawski H M, Roche S, et al. Tuning laser-induced band gaps in graphene. Appl Phys Lett, 2013, 98: 232103

52 Zhou S Y, Gweon G H, Fedorov A V, et al. Substrate-induced bandgap opening in epitaxial graphene. Nat Mater, 2007, 6: 770–775

53 Coletti C, Riedl C, Lee D S, et al. Charge neutrality and band-gap tuning of epitaxial graphene on SiC by molecular doping. Phys Rev B, 2010, 81: 136–138

54 Park J, Mitchel W C, Elhamri S, et al. Observation of the intrinsic bandgap behaviour in as-grown epitaxial twisted graphene. Nat Commun, 2015, 6: 5677

55 Peng X Y, Ahuja R. Symmetry breaking induced bandgap in epitaxial graphene layers on SiC. Nano Lett, 2008, 8: 4464–4468

56 Du A J, Sanvito S, Li Z, et al. Hybrid graphene and graphitic carbon nitride nanocomposite: Gap opening, electron-hole puddle, interfacial charge transfer, and enhanced visible light response. J Am Chem Soc, 2012, 134: 4393–4397

57 Li X R, Dai Y, Ma Y D, et al. Graphene/g-C_3N_4 bilayer: Considerable band gap opening and effective band structure engineering. Phys Chem Chem Phys, 2014, 16: 4230–4235

58 Kan E J, Ren H, Wu F, et al. Why the band gap of graphene is tunable on hexagonal boron nitride. J Phys Chem C, 2012, 116: 3142–3146

59 Mattausch A, Pankratov O. *Ab initio* study of graphene on SiC. Phys Rev Lett, 2007, 99: 076802

60 Nevius M S, Conrad M, Wang F, et al. Semiconducting graphene from highly ordered substrate interactions. Phys Rev Lett, 2015, 115: 136802

61 Varchon F, Feng R, Hass J, et al. Electronic structure of epitaxial graphene layers on SiC: Effect of the substrate. Phys Rev Lett, 2007, 99: 126805

62 Walter A L, Nie S, Bostwick A, et al. Electronic structure of graphene on single-crystal copper substrates. Phys Rev B, 2011, 84: 195443

63 Cho S B, Chung Y C. Bandgap engineering of graphene by corrugation on lattice-mismatched MgO(111). J Mater Chem C, 2013, 1: 1595–1600

64 Huang B, Xu Q, Wei S H. Theoretical study of corundum as an ideal gate dielectric material for graphene transistors. Phys Rev B, 2011, 84: 155406

65 Hunt B, Sanchez-Yamagishi J D, Young A F, et al. Massive dirac fermions and hofstadter butterfly in a van der waals heterostructure. Science, 2013, 340: 1427–1430

66 Wang L, Gao Y D, Wen B, et al. Evidence for a fractional fractal quantum hall effect in graphene superlattices. Science, 2015, 350: 1231–1234

67 Kharche N, Nayak S K. Quasiparticle band gap engineering of graphene and graphone on hexagonal boron nitride substrate. Nano Lett, 2011, 11: 5274–5278

68 Jung J, DaSilva A M, MacDonald A H, et al. Origin of band gaps in graphene on hexagonal boron nitride. Nat Commun, 2015, 6: 6308

69 Giovannetti G, Khomyakov P A, Brocks G, et al. Substrate-induced band gap in graphene on hexagonal boron nitride: *Ab initio* density functional calculations. Phys Rev B, 2007, 76: 073103

70 Moon P, Koshino M. Electronic properties of graphene/hexagonal-boron-nitride moire superlattice. Phys Rev B, 2014, 90: 155406

71 Sachs B, Wehling T O, Katsnelson M I, et al. Adhesion and electronic structure of graphene on hexagonal boron nitride substrates. Phys Rev B, 2011, 84: 195414

72 Slawinska J, Zasada I, Klusek Z. Energy gap tuning in graphene on hexagonal boron nitride bilayer system. Phys Rev B, 2010, 81: 155433

73 Song J C W, Shytov A V, Levitov L S. Electron interactions and gap opening in graphene superlattices. Phys Rev Lett, 2013, 111: 266801

74 Woods C R, Britnell L, Eckmann A, et al. Commensurate-incommensurate transition in graphene on hexagonal boron nitride. Nat Phys, 2014, 10: 451–456

75 Wang E, Lu X, Ding S, et al. Gaps induced by inversion symmetry breaking and second-generation dirac cones in graphene/hexagonal boron nitride. Nat Phys, 2016, 12: 1111–1115

76 Kane C L, Mele E J. Quantum spin hall effect in graphene. Phys Rev Lett, 2005, 95: 226801

77 Boettger J C, Trickey S B. First-principles calculation of the spin-orbit splitting in graphene. Phys Rev B, 2007, 75: 121402

78 Gmitra M, Konschuh S, Ertler C, et al. Band-structure topologies of graphene: Spin-orbit coupling effects from first principles. Phys Rev B, 2009, 80: 235431

79 Abdelouahed S, Ernst A, Henk J, et al. Spin-split electronic states in graphene: Effects due to lattice deformation, rashba effect, and adatoms by first principles. Phys Rev B, 2010, 82: 125424

80 Farjam M, Rafii-Tabar H. Comment on "band structure engineering of graphene by strain: First-principles calculations". Phys Rev B, 2009, 80: 167401

81 Gui G, Li J, Zhong J X. Band structure engineering of graphene by strain: First-principles calculations. Phys Rev B, 2008, 78: 075435

82 Naumov I I, Bratkovsky A M. Gap opening in graphene by simple periodic inhomogeneous strain. Phys Rev B, 2011, 84: 245444

83 Pereira V M, Castro Neto A H, Peres N M R. Tight-binding approach to uniaxial strain in graphene. Phys Rev B, 2009, 80: 045401

84 Ni Z H, Yu T, Lu Y H, et al. Uniaxial strain on graphene: Raman spectroscopy study and band-gap opening. ACS Nano, 2008, 2: 2301–2305

85 Guinea F, Katsnelson M I, Geim A K. Energy gaps and a zero-field quantum hall effect in graphene by strain engineering. Nat Phys, 2010, 6: 30–33

86 Levy N, Burke S A, Meaker K L, et al. Strain-induced pseudo-magnetic fields greater than 300 T in graphene nanobubbles. Science, 2010, 329: 544–547

87 Kotov V N, Uchoa B, Pereira V M, et al. Electron-electron interactions in graphene: Current status and perspectives. Rev Mod Phys, 2012, 84: 1067–1125

Summary for "石墨烯打开带隙研究进展"

Bandgap opening in graphene

XU XiaoZhi[†], YU JiaChen[†], ZHANG ZhiHong[†] & LIU Kaihui[*]

School of Physics, Peking University, Beijing 100871, China
* Corresponding author, E-mail: khliu@pku.edu.cn
† These authors contributed equally to this work

Since the successful exfoliation of graphene monolayer, the exotic and superior electrical properties of graphene have rendered it a promising potential candidate for the future electronics. In particular, the extremely high electron mobility and the rapid developments in mass-fabricating high-quality graphene might initiate a new electronic industry revolution with graphene-based next-generation electronics, namely high-speed field effect transistors (FET). However, the unique Dirac-conical band structure, which provides fascinating electronic features for graphene, turns out to be the primary obstacle that hinders the fabrication of graphene-based FET due to its lack of a band gap. Since a desirably large band gap is required for a high on-off ratio FET, physicists have been trying to figure out ways to open a controllable band gap in monolayer and multilayer graphene from the early stage of graphene research.

Up till now, there are two major kinds of ways towards opening a band gap for graphene. The first is by directly violating the pristine electronic or geometrical properties of graphene, through doping, adatom, introducing periodic defects, constrictions, or other chemical treatments. These methods are generally destructive to graphene's original electronic properties. The other way largely preserves the pristine electronic properties of graphene, such as breaking the intrinsic symmetries of graphene that protect the Dirac cone intact, either through substrate interaction, applying external field, etc., or through other mechanisms such as spin-orbit interaction, strain, and electron many-body effects. There might be multiple mechanisms appearing in various theoretical or experimental works that contribute to the opening of band gap, and this classification is far from clear-cut. Investigations toward this problem include various methodologies, including theoretical proposition, *ab-initio* calculations, density-function or other approximated calculations, and experimental verification using angular resolved photoemission spectroscopic, scanning tunneling spectroscopic and transport evidences. There are also intense theoretical and experimental works on bilayer or multilayer graphene band gap opening.

Although there have been many successful examples of band gap opening in graphene, it is still far to say that graphene-based ideal FET is feasible. The major remaining challenges are increasing the band gap up to a desirable value, making the band gap precisely controllable, and more importantly, preserving the superior electronic properties of graphene. Given that band gap opening is a dramatic change of graphene's electronic structure, it is still not clear which mechanism might ultimately resolve such dilemma, and more investigations are needed in this emergent and fruitful field.

graphene, band gap opening, field-effect transistor (FET)